

Accurate Assessment of Packaging Stress Effects on MEMS Sensors by Measurement and Sensor–Package Interaction Simulations

Xin Zhang, *Member, IEEE*, Seungbae Park, and Michael W. Judy, *Member, IEEE*

Abstract—In this paper, packaging-induced stress effects are assessed for microelectromechanical systems (MEMS) sensors. A packaged MEMS sensor may experience output signal shift (offset) due to the thermomechanical stresses induced by the plastic packaging assembly processes and external loads applied during subsequent use in the field. Modeling and simulation to minimize the stress-induced offset shift are essential for high-precision accelerometers, gyroscopes, and many other MEMS devices. Improvement of plastic package modeling accuracy is accomplished by correlating finite-element analysis package models using measured material properties and package warpage. Using a refined reduced-order MEMS sensor and package interaction model, device offset is simulated, optimized, and compared with data collected from a unique three-axis accelerometer, which uses a single mass for all three axes sensing. As a result, this accelerometer has achieved very low offset ($< 1 \text{ mg}/^\circ\text{C}$) in all XYZ axes over device operation temperature range of -40°C to $+80^\circ\text{C}$. Device offset performance was improved by at least five times after the MEMS design optimization as compared with the one prior to the optimization. [2006-0227]

Index Terms—Finite-element analysis (FEA), MEMS sensor and package interaction (MPI), offset, plastic package, stress, warpage.

I. INTRODUCTION

MICROELECTROMECHANICAL systems (MEMS) sensor products, which utilize displacement measurement, routinely have a full-scale range from a few tens of nanometers to angstroms [1], [2]. Due to this high sensitivity, the device output may deviate from the initial null point due to thermomechanical and mechanical stresses, which can be induced by plastic packaging, assembly processes, and external loads imposed during use in the field. As illustrated in Fig. 1, a plastic-encapsulated MEMS package, which is soldered on the printed circuit board (PCB) via a lead frame, is a composite structure composed of several materials of different thermomechanical properties. The composite nature of the structure generates internal stresses in the package during packaging and assembly processes as well as under thermal

cycling during operation. Without proper design, these stresses can generate sufficient warpage in a MEMS chip to cause offset shifts as well as delamination, cracking, and other failures of the package. It is thus essential to understand and quantify the stresses and warpage for optimal sensor performance and reliability. Accurate sensor performance modeling has been a challenge because of the highly nonlinear and temperature-dependent material properties as well as the subtle interactions between the MEMS sensor and package [3], [4].

Many efforts have been made to predict packaging (particularly encapsulation) and assembly process-induced stresses in plastic packages [5], [10]. These efforts were primarily concentrated on the mechanical deformation and failures in complementary metal–oxide–semiconductor plastic packages, where electrical performance changes due to the package stress were small. If there were stress-sensitive components, they were small and located at the center of the die to minimize the effect. In contrast, the stress effects are critical in MEMS device and package design, where the MEMS device is large relative to the size of the die.

Starting from an accurate measurement of each packaging material's properties and resulting package warpage, this paper presents a detailed procedure of successful package stress management by iterative use of finite-element analysis (FEA) and MEMS sensor and package interaction (MPI) simulations. In the course of this effort, rigorous experimental validation (direct and indirect) of the FEA model has been conducted. The primary objective of this effort is to provide design guidelines of MEMS devices that are less sensitive to packaging-induced stresses and warpage.

II. ITERATIVE METHOD

To accurately predict the stresses in MEMS packages, curing and temperature-dependent constitutive relations for the molding compound and die attach materials are required [5], [6]. Although material properties are available from the vendors, they are usually not sufficient for rigorous analyses. To improve modeling accuracy, an iterative measurement and modeling effort was performed. The material properties were measured at various temperatures. In addition, package warpages were characterized. Using the measured material properties and package warpage, the FEA package model was fine tuned and validated iteratively for further detail analysis of the internal MEMS die stress and warpage. The stress and warpage of the encapsulated MEMS die were imported into the MPI simulator for device

Manuscript received October 20, 2006; revised February 22, 2007. Subject Editor G. Stemme.

X. Zhang and M. W. Judy are with the Micromachined Products Division, Analog Devices, Inc., Cambridge, MA 02139 USA (e-mail: sam.zhang@analog.com; michael.judy@analog.com).

S. Park is with the Department of Mechanical Engineering, State University of New York at Binghamton, Binghamton, NY 13902 USA (e-mail: sbpark@binghamton.edu).

Color versions of one or more of the figures in this paper are available online at <http://ieeexplore.ieee.org>.

Digital Object Identifier 10.1109/JMEMS.2007.897088

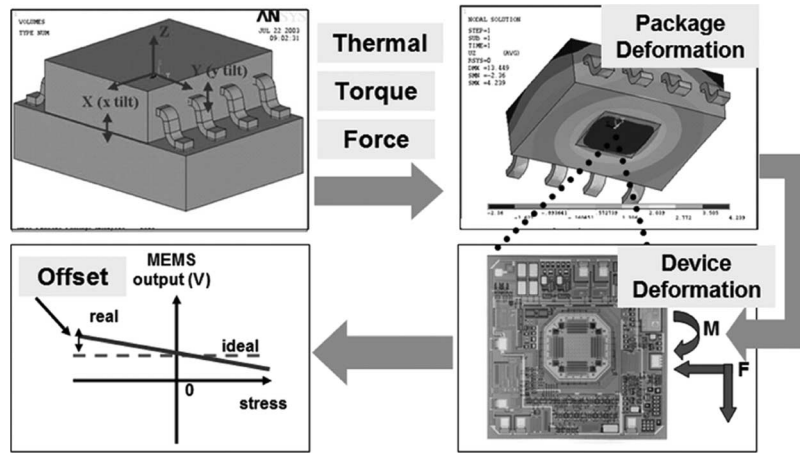


Fig. 1. MEMS sensor output offset induced by packaging stresses in a plastic package.

offset simulation. Finally, the simulations were compared with actual offset characterization for verification. The task was divided by the following five subtasks:

- 1) measurement of package material properties at various temperatures;
- 2) validation and refinement of FEA package models using the measured package warpage;
- 3) prediction of stress and warpage of the encapsulated MEMS die and incorporation of that data into an MPI simulator for offset simulation;
- 4) comparison between measured device offset and MPI simulations;
- 5) MEMS structural design optimization for minimal offset shift.

Throughout this study, package warpage was measured to derive stresses and warpage of a MEMS sensor die, which is not exposed. To compute the correct stress field within the package, it is essential to have a model predicting the package surface warpage accurately. In other words, the warpage measurement was used as a means of validating FEA prediction for package internal stress and warpage distribution.

III. MEMS PACKAGE STRESS AND WARPAGE SIMULATIONS

Fig. 2 shows the packaged accelerometer in a $4 \times 4 \times 1.45$ mm lead-frame chip-scale package (LFCSP) used for this study. The package is composed of MEMS die and its packaging structures die attach, wire bonds, lead frames, and molding compound. The MEMS chip is composed of two functional portions. The central portion is the MEMS sensor structure, which is a micromachined movable structure. The surrounding portion is the integrated sensing electronics. Both the MEMS sensor and circuit are fabricated using the *iMEMS* process of Analog Devices. To protect the fabricated MEMS structures during the plastic encapsulation process and to ensure hermeticity, a silicon cap is placed over the MEMS sensor area using low-temperature glass bonding at the wafer level [7], [8]. The capped dies are then singulated from the wafer and adhered to the die pad of a lead frame using adhesive paste or epoxy.

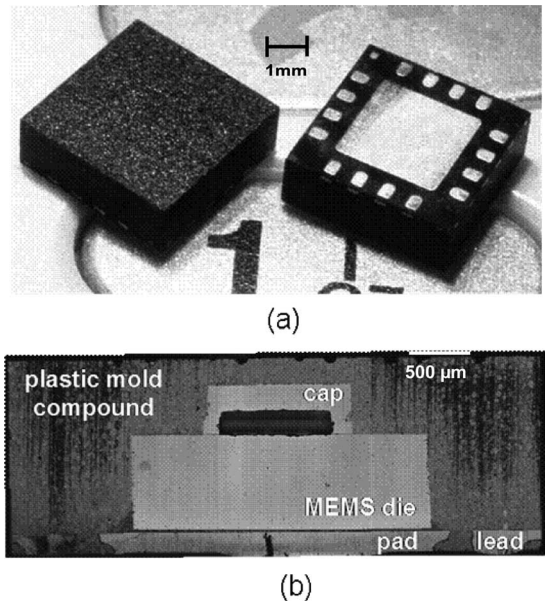


Fig. 2. LFCSP. (a) Top and bottom side views of the $4 \times 4 \times 1.45$ mm LFCSP package. (b) Cross-sectional view of the package.

Then, standard wire-bonding, plastic encapsulation (molding), and package singulation processes are sequentially conducted. The die pad and leads are copper alloys, and the plastic molding compound is a multiaromatic epoxy resin material.

At the molding temperature, the package is essentially stress free with the minor correction of stresses induced by the curing of the molding compound ($\sim 0.2\%$ to 0.3% shrinkage in volume), die attach process, and molding pressure. After curing and cooling down to ambient temperature, the individual package components experience high residual stresses due to the thermal expansion mismatches among the constituents. The MEMS die is under compressive stresses, whereas the molding compound and lead frame are subjected to tensile stresses since the coefficient of thermal expansion (CTE) of silicon MEMS die and cap (2.6 ppm/ $^{\circ}$ C) is much lower than the one of the epoxy molding compound and lead frame (10 – 20 ppm/ $^{\circ}$ C). This difference and the location of the respective parts result in warpage of the entire package.

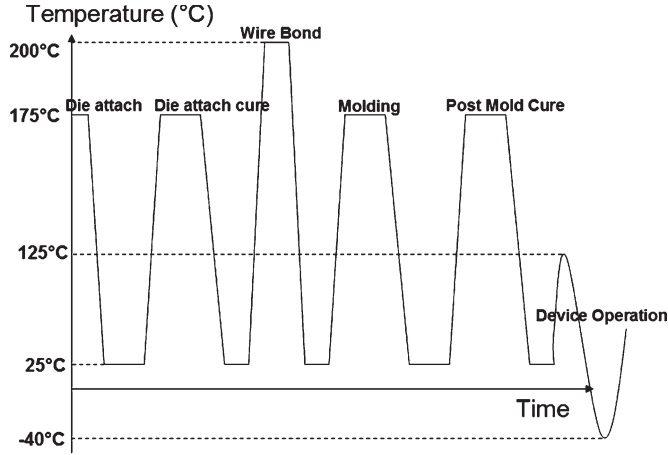


Fig. 3. Thermal loading history of the package assembly processes.

In MEMS plastic packages, the molding compound plays a significant role in package deformation. Its viscoelastic material properties depend on various polymer material compositions and require significant time and effort to be characterized [9]–[11]. FEA models of plastic packages must take into account this property of the molding compound to obtain accurate predictions of package behavior. The viscoelasticity constitutive relation [5], [6] is dependent on the stress–strain history, loading rate, and temperature and is described by a hereditary integral as follows:

$$\sigma(t, T) = 2 \cdot \int_0^t G(t - \tau, T) \cdot \frac{d}{d\tau} \varepsilon_{\text{shear}}(\tau) d\tau + I \cdot \int_0^t K(t - \tau, T) \cdot \frac{d}{d\tau} \varepsilon_{\text{bulk}} d\tau \quad (1)$$

where t is the current time, τ is the past time, T is the current temperature, I is the unit tensor, and G and K are shear and bulk relaxation moduli, respectively, which are functions of t and T .

For most MEMS sensors during normal operations, the ambient temperature change is slow; thus, the transient loading time t effect on the constitutive equation can be negligible. Therefore, the steady-state incremental linear elastic (ILE) method is used to take into account temperature-dependent properties of the fully cured molding compound by accumulating the incremental stresses. The ILE method has been demonstrated to be in good agreement with full viscoelastic calculations for cooling down response [12]. Using a commercial FEA program, i.e., ANSYS, the ILE method is used by applying loads as a series of small incremental load steps, so that the model may follow the temperature-dependent path as closely as possible. The thermal loading history of the LFCSP assembly process is shown in Fig. 3.

During die attach and wire-bonding processes, the molding compound does not exist, and those elements are not activated in the model. At molding temperature (175 °C), the molding compound elements are activated with the initial cure shrinkage of 0.24%. This procedure allows the model to predict stress

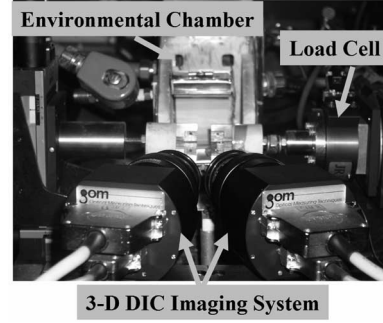


Fig. 4. Setup for nanomechanical characterization system.

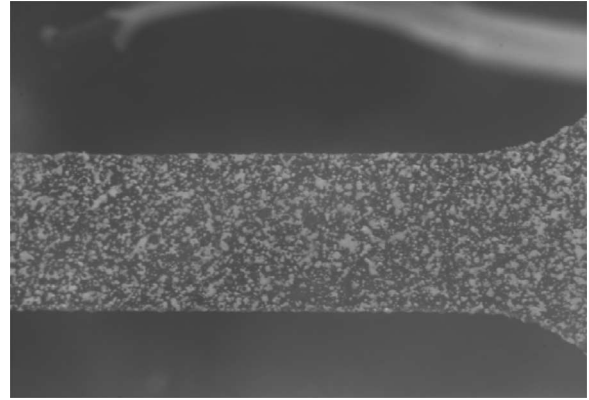


Fig. 5. Prepared dog-bone specimen for tensile test.

history and after-cure warpage accurately. The procedure of simulation process is listed here.

- 1) Turn on the nonlinear solver with Newton–Raphson algorithm and use small load steps for all the sequential simulation process.
- 2) Die attach process: define the global reference temperature as 175 °C. All the molding compound elements are deactivated.
- 3) After the die attach process, cool down the lead frame/die attach/die/cap assembly to 25 °C.
- 4) Wire-bonding process: ramp up the temperature to 200 °C and then cool down to 25 °C.
- 5) Molding process: ramp up the temperature to 175 °C and make the molding compound elements activated (or birth) with initial cure shrinkage. Simulate the whole package assembly at 175 °C to predict the cure shrinkage effect.
- 6) After molding, cool down the assembly to 25 °C.
- 7) Cycle the temperature from –40 °C to 125 °C and record stress and warpage.

IV. MATERIAL PROPERTIES AND PACKAGE WARPAGE MEASUREMENT

For the material property measurements, traditional tensile tests were performed using a nanomechanical characterizer, which is composed of a nanoscale tensile tester (positional sensitivity of 10 nm) and a 3-D digital image correlation (DIC) system used as a full-field optical strain gauge [13]. The 3-D DIC, which is a form of photogrammetry, is a noncontact full-field optical deformation measurement technique in which the

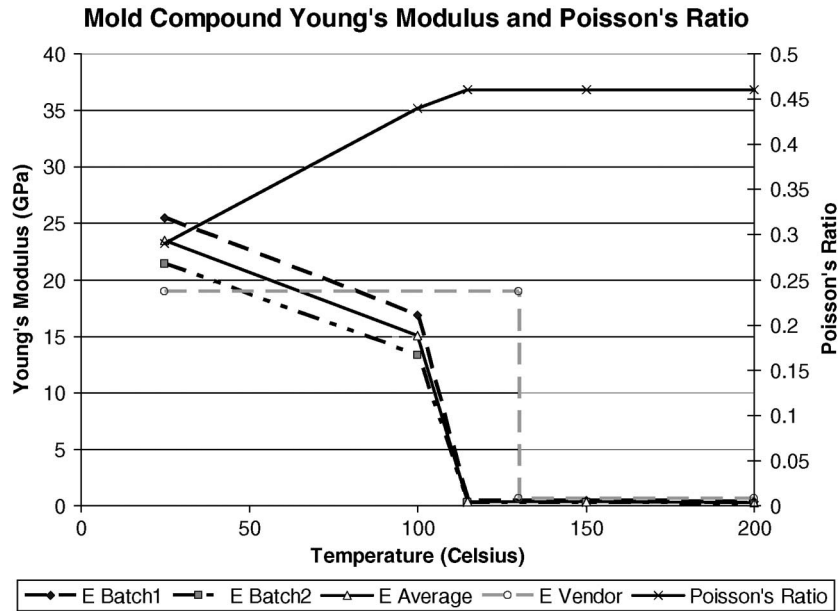


Fig. 6. Molding compound elastic modulus and Poisson's ratio with respect to temperature.

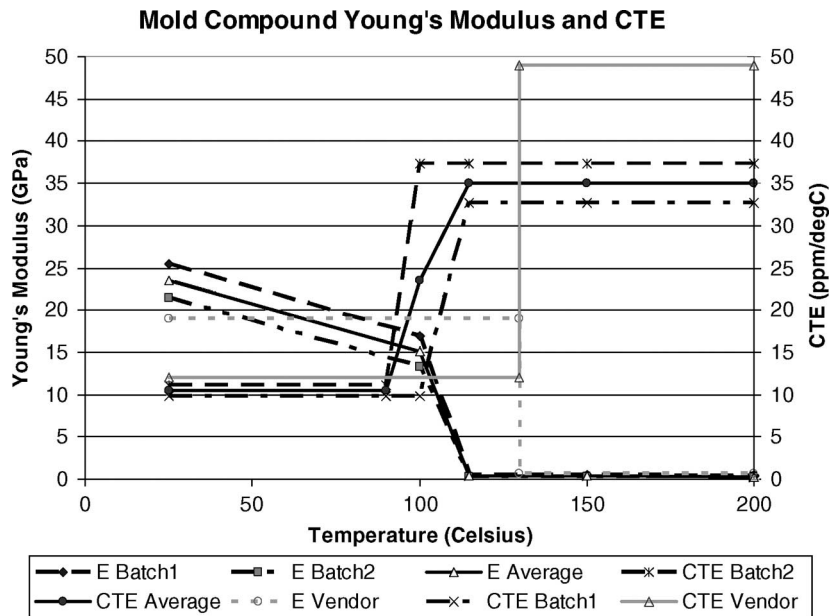


Fig. 7. Molding compound elastic modulus and CTE with respect to temperature.

surface features of the object are traced in digital images. Due to the capability of the full-field strain mapping, Young's modulus and Poisson's ratio were measured simultaneously. Fig. 4 shows the setup of the integrated system with an environmental chamber that allows the measurement in the temperature from $-55\text{ }^{\circ}\text{C}$ to $300\text{ }^{\circ}\text{C}$. Using the setup, package warpage can also be characterized at various temperatures.

A. Molding Compound and Die Attach Material Properties

A tensile test specimen was temporarily fixed at both ends by instant glue and subsequently tightened by a grip to prevent the initial misalignment and slippage during loading at an elevated temperature. To avoid the grip constraint effect, the full-field

strain at the test section of dog-bone specimen was carefully investigated, and the data were extracted at the uniformly deformed section. To create a random variation of gray scale on the specimen, very thin and small black and white paint speckles were sprayed on the specimen, as shown in Fig. 5. The use of black and white speckles is to enhance the contrast of the image for image correlation. Thousands of unique correlation facets are defined across the imaging area, where the center of each facet is considered as a measurement point that can be thought of as an extensometer or strain rosette. These facet centers are traced with an accuracy of up to 100th of a pixel.

The measured Young's moduli for molding compounds from different batches are plotted as a function of temperature in Fig. 6. The glass transition temperature T_g for the molding

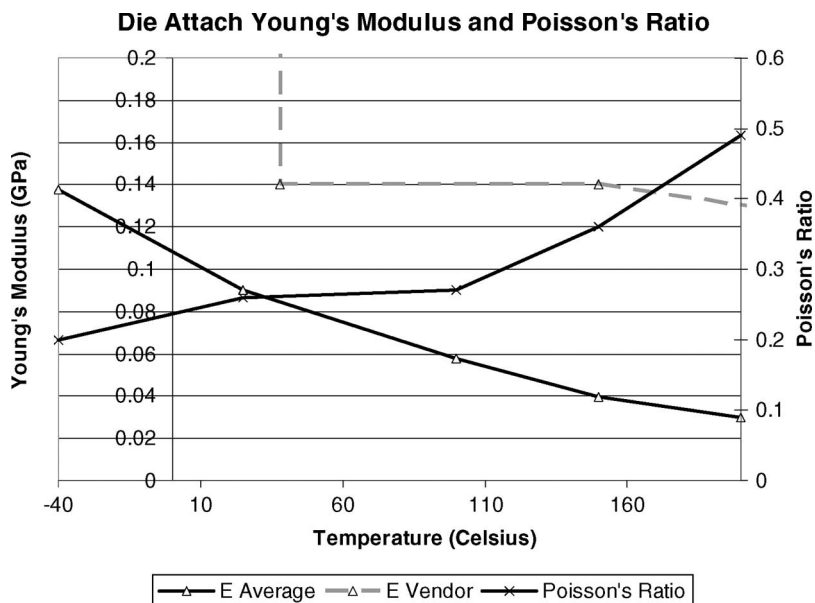


Fig. 8. Young's modulus and Poisson's ratio of a die attach material with respect to temperature.

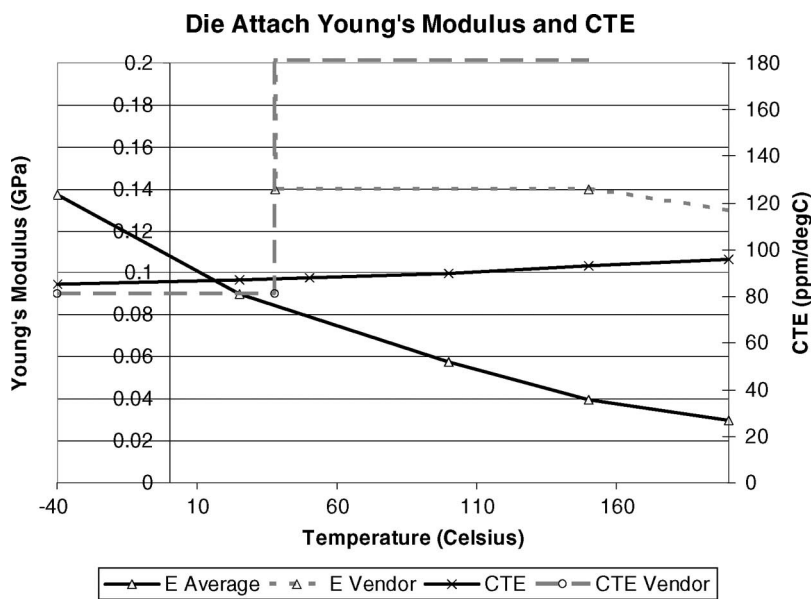


Fig. 9. Young's modulus and CTE of a die attach material with respect to temperature.

compound is about 110 °C. Above T_g , as expected, the modulus becomes very low (about 0.5 GPa), whereas it is much higher (about 20 GPa) below T_g . The CTE variation with respect to temperature for the same materials is plotted in Fig. 7. It is clear that Poisson's ratio also changes with respect to T_g . It is observed that a batch of lower CTE has a higher Young's modulus. This can be explained by the difference of filler contents. Increasing filler content in the molding compound reduces thermal stresses in a package by reducing the CTE. However, there is a counteracting effect of increasing the effective elastic modulus, which increases thermal stresses. The two effects must be carefully considered in the selection of appropriate package materials.

The measured variation of Young's modulus and CTE of a die attach material with respect to temperature are plotted in

Figs. 8 and 9, respectively. Both Young's modulus and CTE show smooth variation regardless of the T_g . According to the vendor's data sheet, the T_g is around 40 °C. Generally speaking, Young's modulus is a more important property for an adhesive since it defines the degree of coupling between the die and the lead frame in a package.

B. In Situ Package Warpage Measurement

Warpage measurements were conducted on packages selected randomly from different assembly lots to account for process variations. The *in situ* 3-D DIC measurement setup was used to measure warpage of both top and bottom sides (lead frame side) of the package over a temperature range of -55 °C to 200 °C. The 200 °C condition is beyond normal

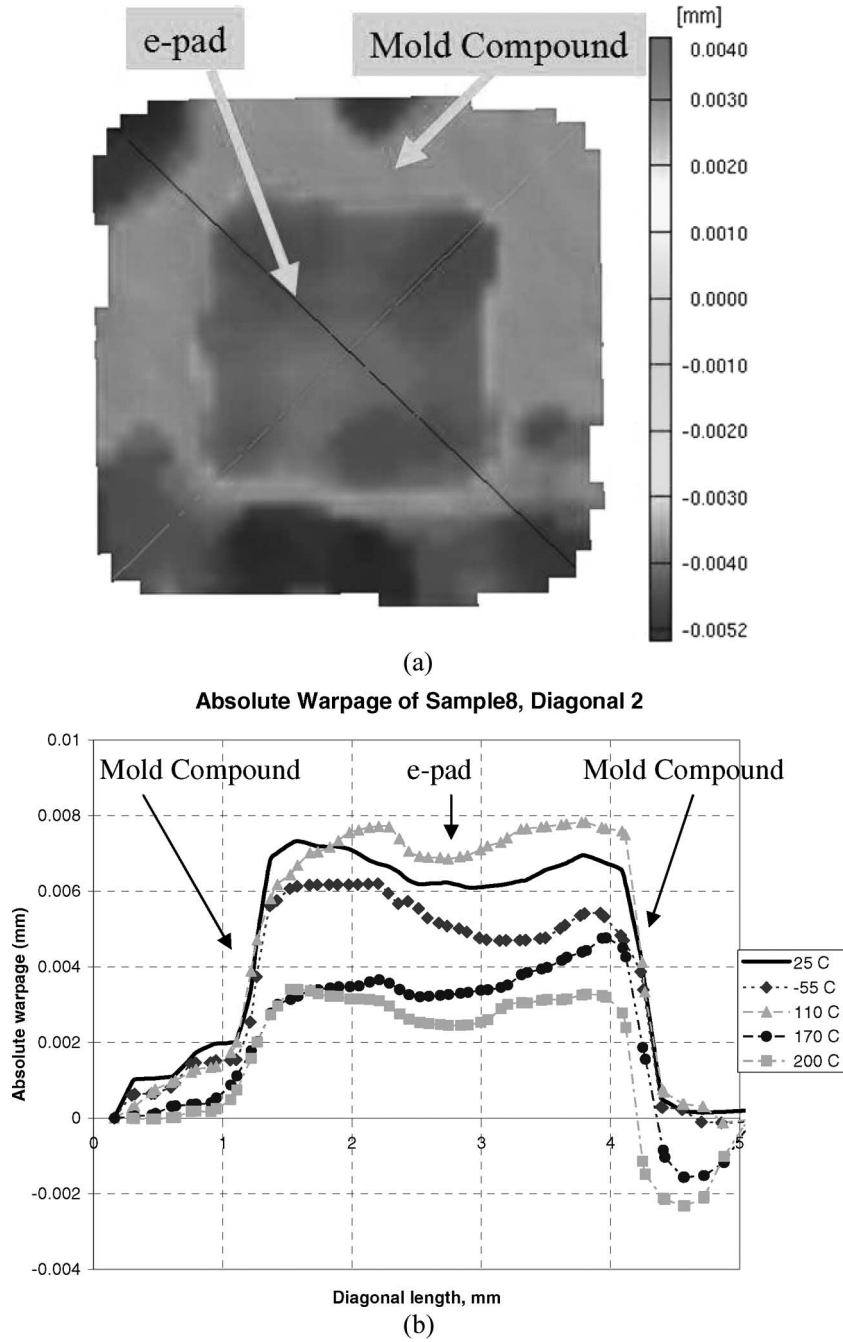


Fig. 10. (a) Package warpage contour plot of the e-pad side at room temperature (25 °C). With exposed lead frame side facing up (+Z), positive warpage indicates surface displacing up in the +Z-axis. (b) Warpage plot over -55 °C to 200 °C along a diagonal of the package. The e-pad sticks out of the package as a result of the mold shrinkage.

application and testing range, and this condition was measured only for reliability interest under solder reflow condition, which is usually at about or over 200 °C. Fig. 10 shows a warpage contour plot at room temperature [Fig. 10(a)] and linear plots along the two diagonals with respect to various temperatures [Fig. 10(b)]. The warpage is defined by the difference of out-of-plane displacement between the package center and corners. As expected, the package center, where the exposed lead frame pad (e-pad) sticks out (convex), is as much as 7 μm as compared to the package corners due to the cure shrinkage of the molding compound and subsequent cooling down to the room temperature. In the mean time, within the e-pad, the corner

is up compared to the middle portion. The package warpage increased at lower temperatures but reduced considerably at the temperature beyond 110 °C (*T_g*) due to the low molding compound modulus and low e-pad warpage as temperatures approaching the molding temperature.

V. FEA MODELING AND COMPARISON WITH MEASUREMENT

For the validation of the FEA model, measured and simulated warpages were compared. In the comparison, e-pad warpage was utilized as a key parameter since the MEMS die is mounted

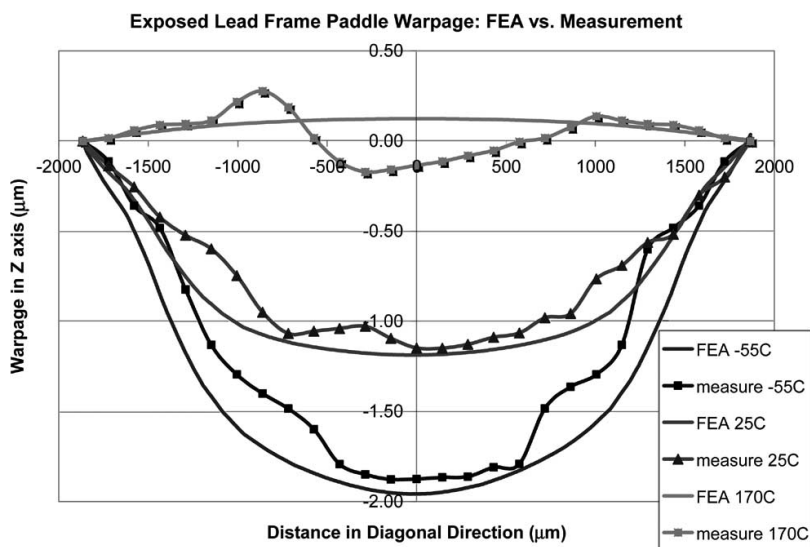


Fig. 11. Comparison of FEA prediction and measurement of lead frame warpage. The measurement data were leveled off with respect to the lead frame bottom surface to differentiate the pure lead frame warpage from the expansion and tilt of the whole package shown in Fig. 10(b).

by die attach onto the lead frame pad inside the plastic package. After the validation of the model with the e-pad warpage, prediction of the MEMS die stress and warpage was conducted. The results were used as an input to the MPI simulator to simulate the MEMS device offset behavior.

For the 3-D FEA model, the measured temperature-dependent material properties of molding compound, die attach, and lead frame were used. Fig. 11 shows the comparison of the relative e-pad only warpage along a diagonal axis of the e-pad between FEA model prediction and measurement. Negative warpage indicates a concave-shaped lead frame (center down into the package when it is viewed from the e-pad side). At the molding temperature (175 °C), the difference is greater because the transition of Young's modulus and CTE is very sensitive to temperature and process variations, and these variations are difficult to be captured in simulations. However, the absolute amount of discrepancy is negligible since the overall warpage at and above T_g is quite small and does not impact the device performance significantly. Die warpage is much greater at lower temperature (−55 °C), thus causing the MEMS device to have the largest offset. Thus, the lower temperature regime is much more critical to device performance than higher temperatures. It turned out that the FEA predictions and measurements were in very good agreement in the lower temperature range, with a discrepancy of less than 5%.

Fig. 12(a) shows a full plastic package solid model with the integration of a MEMS sensor for clarification of its location. Using the validated FEA package model, die stress and warpage are predicted. Fig. 12(b) shows a cross-sectional contour plot of package warpage and a component of in-plane stress (σ_{xx}) at 25 °C. It is observed that the whole package warps upward due to the shrinkage of the molding compound and the sequential cooling down process. Accordingly, the lead frame is under tensile stress, and the MEMS die is under compressive stress. Details of MEMS die stress and warpage are extracted along a path on the top surface of the die, as shown in Fig. 12 (dashed line), using the path's endpoints as zero warpage reference

points. The maximum die warpage decreases from 0.2 to almost 0 μm as temperature increases from −40 °C to 175 °C (Fig. 13). The die surface stress plot (Fig. 14) shows that the stress changes from −45 MPa (compressive) to almost 0 MPa over the same temperature range. At lower temperatures, both die stress and warpage are larger, and accordingly, the MEMS device offset is expected to be bigger. This prediction agrees with measured devices, which will be discussed in the next section. It should be noted that both stress and warpage curves show nonlinear behavior in the device operation temperature range of −40 °C to 125 °C. The die warpage is predominately induced by the lead frame deformation, whereas the die surface compressive stress is predominately induced by the mold compound compression. Therefore, the molding compound nonlinear T_g effect is not clearly seen in Fig. 13, which is the plot for the die warpage. However, the compressive die stress T_g effect can be clearly seen in Fig. 14 due to the molding compound compression.

VI. MPI SIMULATIONS AND DEVICE OFFSET OPTIMIZATIONS

The die stress and warpage that were obtained by FEA simulation were incorporated into a newly developed MPI simulator using reduced-order electromechanical models provided by CoventorWare, which is a commercially available MEMS design software supplied by Coventor, Inc. The reduced-order electromechanical sensor model can be used to study the sensor's static and dynamic characteristics such as static or transient mechanical response and sensitivity analyses. By applying die stress and warpage to the MPI model, the sensor behavior over temperature can be simulated. This paper focuses on the offset response over temperature.

MEMS device offset is usually characterized by “zero-g” output voltage shift over temperature without any acceleration imposed to the part. When MEMS microfabrication is complete, the MEMS devices are probed at wafer level and

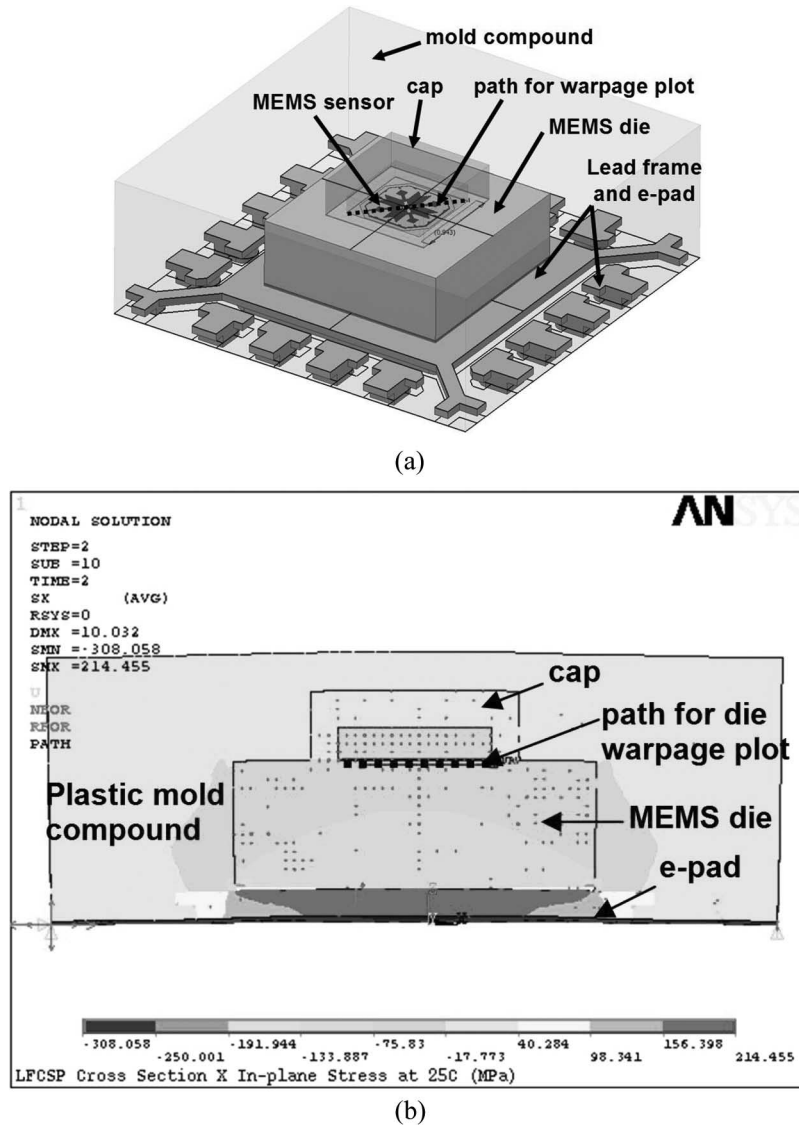


Fig. 12. Package solid model and FEA simulation results. (a) Full plastic package solid model for the FEA simulation. (b) Cross-sectional view of package warpage and the X-axis in-plane stress σ_{xx} at 25 °C.

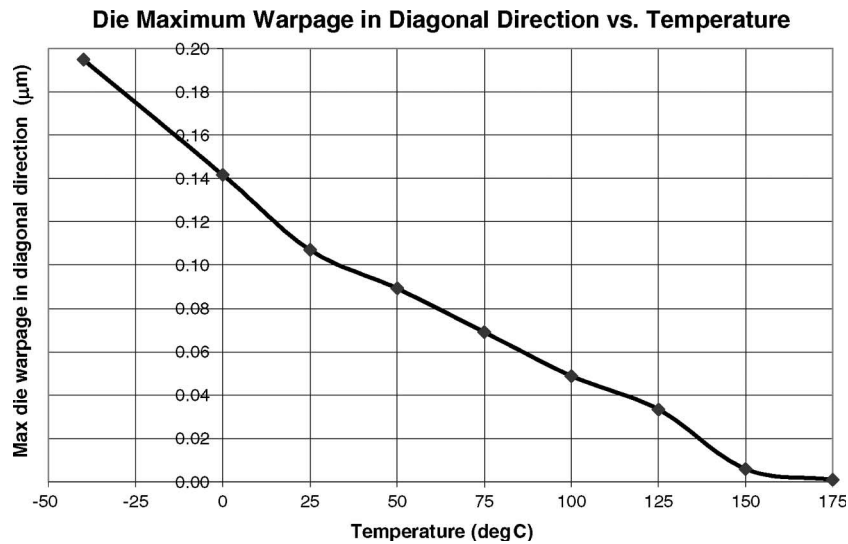


Fig. 13. Maximum warpage of the die along a diagonal with respect to temperature.

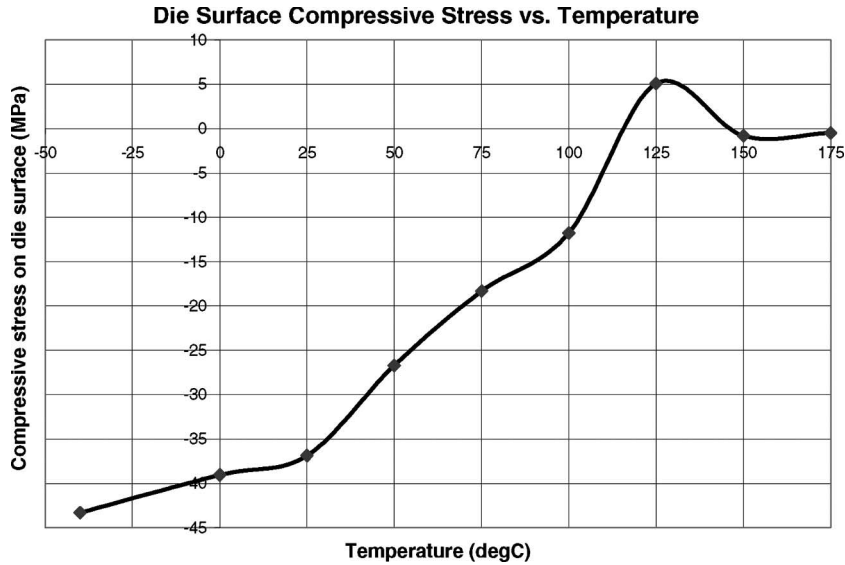


Fig. 14. Die surface in-plane stress σ_{xx} with respect to temperature.

trimmed to a zero-g “null” output voltage (usually $VDD/2$). During subsequent assembly processes such as die attach curing, plastic overmolding, and solder reflow, the MEMS device in the package experiences thermomechanical stresses. As a result, the zero-g output is changed from the trimmed value. The zero-g offset shift at various temperatures is measured by placing a MEMS package, which has been soldered on a PCB, into a temperature-controlled chamber for thermal cycling. Temperature ranges from $-40\text{ }^{\circ}\text{C}$ to $125\text{ }^{\circ}\text{C}$ or from $-25\text{ }^{\circ}\text{C}$ to $80\text{ }^{\circ}\text{C}$ are typical in automotive or consumer electronics applications, respectively.

Fig. 15(a) and (b) shows a scanning electron microscopy photo of MEMS three-axis accelerometer fabricated in the *iMEMS* process. This newly developed three-axis accelerometer uses single mass for all three axes sensing and integrates with signal processing electronics on the same chip. The *Z*-axis acceleration output relies on direct sensing of capacitance change between the movable polysilicon mass and the polysilicon ground plane fabricated on top of the silicon substrate. The warpage of the MEMS die changes the sensing gap between the movable mass and the ground plane and, in turn, changes the *Z*-axis sensing capacitance and, thus, shifts the zero-g offset. To minimize this offset, a straightforward solution is minimizing the packaging-induced stresses and/or warpage. However, this approach requires the CTE of the molding compound and lead frame materials to be close to the CTE of silicon ($2.6\text{ ppm}/^{\circ}\text{C}$) and is not practical. In this paper, another approach was pursued. Now with a thorough understanding of the package behavior along with a well-validated FEA model, the key MEMS mechanical structures, such as the location of the spring anchors and the length of the support arms, were meticulously engineered to make the sensing capacitance and referencing capacitance insensitive to package stress and warpage change.

As a first step, the die warpage and stresses obtained by FEA simulation are curved fitted and lumped into the MPI sensor models based on the reduced-order elements provided by CoventorWare. As an outcome of Coventor/Analog Devices

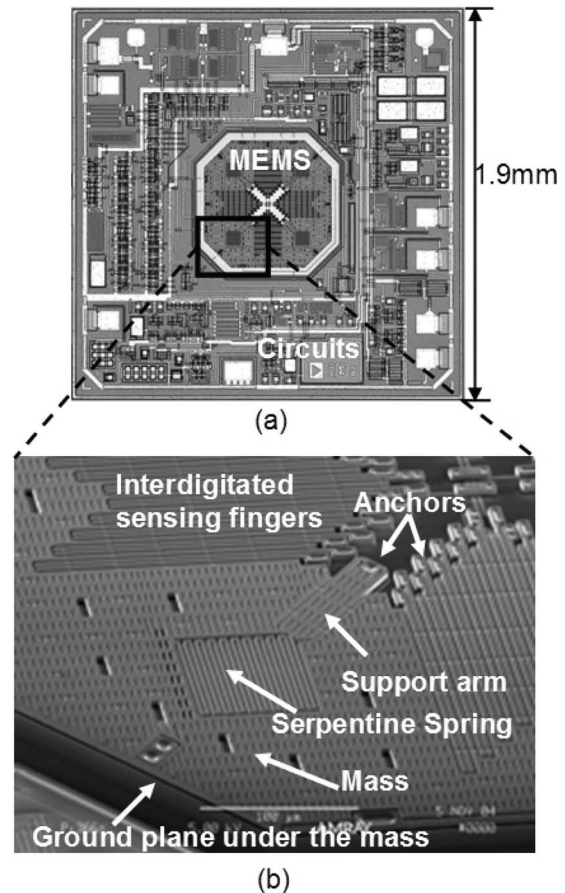


Fig. 15. (a) MEMS three-axis accelerometer fabricated in the *iMEMS* process from Analog Devices. (b) Magnified view of a quarter of the MEMS structure. Two fixed fingers and one sensing finger are interdigitated for the differential capacitive measurements during accelerations in the *X*-axis or *Y*-axis. *Z*-axis sensing relies on direct sensing of capacitance change between the movable polysilicon mass and the ground plane fabricated on top of the silicon substrate.

joint research and development, the CoventorWare *Architect* module now provides new reduced-order elements such as deformable anchors, electrode plates, and comb drives. Through

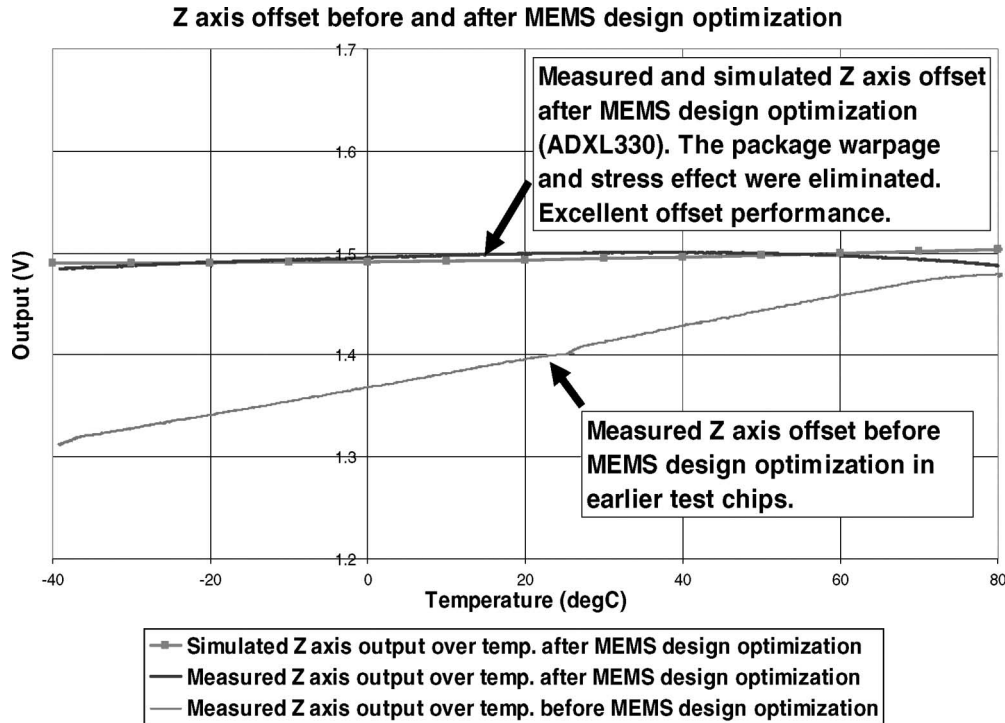


Fig. 16. Three-axis accelerometer Z-axis offset before and after MEMS design optimization.

these deformable elements, the package/die warpage and stress effects can be directly imparted to the reduced-order sensor model in CoventorWare. The sensing capacitance can then be accurately simulated with complete consideration of the MEMS structure mechanical stiffness, die warpage and stress, electrostatic forces, and fringing fields. Z-axis sensing usually utilizes a referencing capacitor with differential sensing mechanism for better offset balance. The capacitance changes of the referencing capacitor can be modeled using the same method. By carefully designing the key MEMS structures, e.g., the shape and dimension of the sensing and referencing capacitors, the location of the spring anchors, and the length of the support arms, an optimum sensor design can be found so that the sensing capacitance and the referencing capacitance have no change or the same change over temperatures from their nominal values, respectively. In this way, the Z-axis output signal is made insensitive to package stress and warpage. Similarly, X-axis and Y-axis output offset can be minimized using the same optimization method through MPI simulations.

Fig. 16 shows the measured Z-axis offset before and after the MEMS design optimization on key structures, as mentioned previously in the text. Prior to the optimization, the sensor exhibited large offset over temperature. Using the current design methodology incorporated with the MPI simulations, a new three-axis accelerometer (ADXL330) is successfully developed. The sensor is optimized to minimize the stress and warpage effects. As a result, it has achieved a very low offset in all XYZ axes over the entire device operation temperature range of -40°C to $+80^{\circ}\text{C}$. The offset over temperature is less than $1\text{ mg}/^{\circ}\text{C}$, with a nominal sensitivity of 0.3 V/g at 3-V supply. The $< 1\text{ mg}/^{\circ}\text{C}$ offset is equivalent to only 1-nm MEMS mass displacement error from -40°C to $+80^{\circ}\text{C}$. This is a tiny

residue after the cancellation of over $0.2\text{-}\mu\text{m}$ die warpage and additional stresses. Device offset performance was improved by at least five times after the MEMS design optimization as compared with the one prior to the optimization. It is noted that model prediction and measurement of offset agree very well for all the cases (both before and after optimization).

VII. CONCLUSION

To design low-offset MEMS devices and accurately assess packaging stress effects on device performance in plastic overmold packages, iterative methods integrating measurement techniques, FEA modeling, and MPI simulations were performed. FEA modeling of a package using accurately measured temperature-dependent material properties showed very good agreement with measured warpage in various temperatures. The validated FEA models were used to predict MEMS die stress and warpage. The device offset performance was simulated by using MPI simulation system. The final correlation on the three-axis accelerometer showed that its offset behavior correlates with modeling very well. As a result of this study and MPI simulation, the optimized three-axis accelerometer showed excellent offset improvement over its previous designs and achieved less than $1\text{ mg}/^{\circ}\text{C}$ offset over temperature performance in all three axes.

REFERENCES

- [1] M. W. Judy, "Evolution of integrated inertial MEMS technology," in *Proc. Solid-State Sensor, Actuator, and Microsystems Workshop*, Hilton Head Island, SC, Jun. 2004, pp. 27–32.
- [2] C. H. Yun, X. Zhang, J. Kuang, Y. Xu, and J. A. Geen, "Stress minimization in ceramic MEMS gyroscope packages," in *Proc. IMAPS*, Long Beach, CA, Nov. 2004, Session WP3-3.

- [3] S. Fischer, T. Fellner, J. Wilde, H. Beyer, and R. Janke, "Analyzing parameters influencing stress and drift in moulded hall sensors," in *Proc. 1st Electron. Syst. Integration Technol. Conf.*, Sep. 2006, pp. 1378–1385.
- [4] X. Zhang, S. B. Park, R. Navarro, and M. W. Judy, "Accurate assessment of packaging stress effects on MEMS devices," in *Proc. 10th IThERM*, May 30–Jun. 2, 2006, pp. 1336–1342.
- [5] R. Darveaux, L. Norton, and F. Carney, "Temperature dependent mechanical behavior of plastic packaging materials," in *Proc. 45th Electron. Compon. and Technol. Conf.*, May 1995, pp. 1054–1058.
- [6] K. M. B. Jansen, L. Wang, C. van't Hof, L. J. Ernst, H. J. L. Bressers, and G. Q. Zhang, "Cure, temperature and time dependent constitutive modeling of moulding compounds," in *Proc. 5th Int. Conf. Thermal and Mech. Simul. and Experiments Microelectron. and Microsyst., EuroSim*, 2004, pp. 581–585.
- [7] L. E. Felton, M. Duffy, N. Hablutzel, P. W. Farrell, and W. A. Webster, "Low-cost packaging of inertial MEMS devices," in *Proc. IMAPS*, Boston, MA, Nov. 2003, pp. 402–406.
- [8] C. H. Yun, X. Zhang, W. A. Webster, T. Lor, and E. S. Lacsamana, "Micromachined accelerometer performance in plastic overmold packages," in *Proc. IMAPS*, Philadelphia, PA, Sep. 2005, pp. 143–147.
- [9] J. S. Kim, K. W. Paik, S. H. Oh, and H. S. Seo, "Thermo-mechanical stresses in laminated polymer films on silicon substrates," in *Proc. 7th Int. Conf. Multichip Modules and High Density Packaging*, Apr. 1998, pp. 449–453.
- [10] J. W. Y. Kong, J. K. Kim, and M. F. Yuen, "Warpage in plastic packages: Effects of process conditions, geometry and materials," *IEEE Trans. Electron. Packag. Manuf.*, vol. 26, no. 3, pp. 245–252, Jul. 2003.
- [11] G. Kelly, C. Lyden, W. Lawton, J. Barrett, A. Saboui, H. Pape, and H. J. B. Peters, "Importance of molding compound chemical shrinkage in the stress and warpage analysis of PQFP's," *IEEE Trans. Compon., Packag., Manuf. Technol. B*, vol. 19, no. 2, pp. 296–300, May 1996.
- [12] R. B. R. van Silfhout, J. G. J. Beijer, K. Zhang, and W. D. van Driel, "Modelling methodology for linear elastic compound modelling versus visco-elastic compound modeling," in *Proc. 6th Int. Conf. Thermal, Mech. and Multi-Physics Simul. and Experiments Micro-Electron. and Micro-Syst., EuroSim*, Apr. 2005, pp. 483–489.
- [13] S. B. Park, S. Chung, H. Ackler, S. Mahkar, and P. Lin, "Structural reliability of SU-8 material for MEMS application," in *Proc. ASME IMECE*, Nov. 2005, pp. 251–258.



Xin Zhang (S'99–M'01) received the B.S. degree in precision optical engineering and the B.A. degree in technical communication from Tsinghua University, Beijing, China, in 1997 and 1998, respectively, and the M.S. degree in mechanical engineering, with a focus on micro electro mechanical systems (MEMS) design, from George Washington University, Washington, DC, in 2001.

He is a Senior MEMS Design Engineer in the Micromachined Products Division, Analog Devices, Inc. (ADI), Cambridge, MA. In the past six years of working at ADI, he has been a key microstructure designer for the company's high-performance MEMS accelerometers, optical switches, microphones, and other products. He, together with Dr. M. W. Judy, designed the MEMS structures of the innovative single-mass sensing three-axis accelerometers ADXL330. In addition to designing and optimizing MEMS sensors, he is also an expert in modeling MEMS packages and sensor–package interactions. He has about ten U.S. patents pending and many other technical publications.

Mr. Zhang has chaired MEMS sessions and given invited presentations at international conferences. He was the recipient of the Best Paper Award at the IEEE IThERM 2006 Conference and one of the recipients of ADI's Award in 2007 for excellence in product development.



Seungbae Park received the Ph.D. degree from Purdue University, West Lafayette, IN, in 1994.

He began his professional career at the IBM Microelectronics Division, Endicott, NY, as a Development Engineer. Later, he was engaged in the reliability engineering responsible for the reliability of IBM's corporate flip-chip technology in both leaded and lead-free solders and high-performance packaging. After seven years at IBM, he started his academic career at the State University of New York at Binghamton in 2002. He has more than 60 technical publications. He is the holder of four U.S. patents. His research interests include physical reliability for microelectronics and micro electro mechanical systems (MEMS) packaging.

Dr. Park has served on several technical committees, including the JEDEC 14-1 Reliability Committee. He has been chairing iNEMI's Modeling and Simulation Technical Work Group, "Electronics Packaging" council in the Society of Experimental Mechanics, and "Emerging Technology" track for IThERM 2006. He is currently the "Electronics and Photonics Packaging" Division Representative of IMECE 2007.



Michael W. Judy (S'87–M'94) received the B.S. degree from Massachusetts Institute of Technology, Cambridge, in 1987, and the Ph.D. degree from the University of California, Berkeley, in 1994. In his doctoral research, he was the first to demonstrate polysilicon sidewall beams as structural elements in microresonators and microactuators.

In 1993, he joined Analog Devices, Inc. (ADI), where he has participated in all aspects of micro-electromechanical system (MEMS) processing, design, and manufacturing. In 2003, he was promoted to an ADI Fellow, which is the highest technical level within ADI. He is currently the MEMS Design Manager for the Micromachined Products Division, ADI, Cambridge, MA, where he and his group have developed many accelerometers, gyros, optical switches, microphones, and other products. He has over 20 U.S. patents pending or awarded. His research interests include microsensors and microactuator design and modeling, design for manufacturing methodologies, and next-generation process and packaging technologies.

Dr. Judy has served on several technical committees, including most recently on the Technical Program Committee for Transducers 2007.